Field-Induced Magnetic Order in Quantum Spin Liquids

Stefan Wessel,[1,2] Maxim Olshanii,[1] and Stephan Haas[1]

[1]*Department of Physics and Astronomy, University of Southern California, Los Angeles, California 90089-0484*

[2]*Institut für Theoretische Physik, ETH-Hönggerberg, CH-8093 Zürich, Switzerland*

(Received 24 May 2001; published 30 October 2001)

We study magnetic-field-induced three-dimensional ordering transitions in low-dimensional quantum spin liquids, such as weakly coupled, antiferromagnetic spin-1/2 Heisenberg dimers and ladders. Using stochastic series expansion quantum Monte Carlo simulations, we obtain the critical scaling exponents which dictate the power-law dependence of the transition temperature on the magnetic field. These are compared with recent experiments on candidate materials and with predictions for the Bose-Einstein condensation of magnons. The critical exponents deviate from isotropic mean-field theory and exhibit different scaling behavior at the lower and upper critical magnetic fields.

DOI: 10.1103/PhysRevLett.87.206407 PACS numbers: 75.10.Jm, 75.30.–m, 75.50.Ee

Many low-dimensional quantum spin liquids, such as antiferromagnetic Heisenberg spin ladders, have a nonmagnetic valence-bond ground state with a finite energy gap to the lowest band of triplet excitations. This spin gap can be suppressed by an applied magnetic field. Increasing the external field beyond a critical value h_{c1} leads to partial spin polarization and incommensurate, gapless excitations. A second transition occurs at a higher critical field, h_{c2}, above which the system becomes fully polarized. It has been suggested that in the partially polarized phase, $h_{c1} < h < h_{c2}$, weak couplings between the low-dimensional subsystems induce a three-dimensional (3D) condensation of magnetic excitations at low temperatures [1,2].

Indications of such 3D ordering transitions induced by external magnetic fields were observed by high-field nuclear magnetic resonance and inelastic neutron scattering measurements on the quantum spin liquids $TlCuCl_3$ [3,4] and $Cu_2(C_5H_{12}N_2)_2Cl_4$ [5–8]. The crystal structure of $TlCuCl_3$ suggests that this compound consists of weakly coupled Cu_2Cl_6 dimers, involving two neighboring spin-1/2 Cu^{2+} ions in its b-c plane [9,10]. A small spin gap of $\Delta \approx 7.5$ K was determined from measurements of the magnetic susceptibility [3,11]. On the other hand, $Cu_2(C_5H_{12}N_2)_2Cl_4$ is generally viewed as a compound of weakly coupled two-leg ladders with intraladder exchange constants $J_\perp \approx 13.2$ K, $J_\parallel \approx 2.5$ K, and a spin gap $\Delta \approx 10.5$ K [5]. However, a very recent study has concluded that this material consists of frustrated planar networks of dimers [12].

We may further expect field-induced 3D ordering phenomena to occur in $(C_5H_{12}N)_2CuBr_4$ [13]. This compound is believed to consist of weakly coupled two-leg ladders with a strong rung coupling, $J_\perp \simeq 13.3$ K, between adjacent $CuBr_4$ tetrahedra, and a weaker coupling, $J_\parallel \simeq 3.8$ K, along the legs of the ladders [14]. Its spin gap was observed to be $\Delta \approx 9.5$ K.

Whatever the effective dimensionalities of these compounds may turn out to be [$d = 0$ for $TlCuCl_3$, $d = 1$ or $d = 2$ for $Cu_2(C_5H_{12}N_2)_2Cl_4$, and $d = 1$ for $(C_5H_{12}N)_2CuBr_4$], they share the essential common feature of a spin-liquid ground state and a small but finite spin gap that can be overcome by presently accessible magnetic fields.

From the theoretical side, it has been proposed that the observed field-induced 3D magnetic ordering transition in these systems can be interpreted as a Bose-Einstein condensation (BEC) of magnons, resulting in a staggered, transverse magnetic order [1,15–17]. This class of quantum phase transition is characterized by a critical exponent α, which relates the ordering temperature T_c to the applied magnetic field according to

$$T_c(h) \propto |h - h_c|^{1/\alpha}. \tag{1}$$

The exact determination of this power-law dependence from experimental data turns out to be somewhat delicate, because it requires simultaneous fitting of the critical field and the scaling exponent. Furthermore, the number of data points tends to be sparse in the scaling regime around (h_c, T_c). Nevertheless, the experimentally deduced exponents, $\alpha \approx 2.0$ for $TlCuCl_3$ and $\alpha \approx 1.5$ for $Cu_2(C_5H_{12}N_2)_2Cl_4$, appear to be within the general range of the value $\alpha_{\mathrm{IBEC}} = 3/2$, expected from isotropic Bose-Einstein Hartree-Fock theory [1,15,16]. However, material-specific details such as spin-phonon coupling and magnetic frustration in these compounds are likely to influence the precise values of the scaling exponents.

In this Letter, we address the fundamental question of obtaining these critical scaling properties directly from microscopic models of weakly coupled low-dimensional quantum spin systems. We apply the recently developed stochastic series expansion quantum Monte Carlo (QMC) technique [18] to the 3D antiferromagnetic spin-1/2 Heisenberg model with spatially anisotropic exchange couplings,

$$H = \sum_{\langle i,j \rangle} J_{ij} \mathbf{S}_i \cdot \mathbf{S}_j - h \sum_i S_i^z, \tag{2}$$

where h denotes the applied magnetic field. The relative strengths of the nearest-neighbor exchange coupling constants J_{ij} are illustrated in Fig. 1, in which planar sections of two clusters with different configurations of J_{ij} are shown. Figure 1(a) illustrates an ensemble of weakly coupled dimers oriented along the x direction, a configuration resembling the minimal effective magnetic structure of $TlCuCl_3$. Figure 1(b) shows a quasi-1D array of weakly coupled two-leg Heisenberg ladders oriented along the y direction, as may be realized in $(C_5H_{12}N)_2CuBr_4$ or $Cu_2(C_5H_{12}N_2)_2Cl_4$.

The numerical algorithm involves expansions of the partition function in inverse temperature, uses local and global system updates, and is significantly more efficient than conventional QMC schemes. In this work we study cubic lattices with up to $10 \times 10 \times 10$ quantum spins down to very low temperatures, by which is meant less than 1% of the exchange coupling strength J which sets the scale of the problem. Moreover, the stochastic series expansion QMC method can handle external magnetic fields of any strength without the problems common to world line QMC techniques, such as the QMC loop algorithm.

In Fig. 2(a), the low-temperature regime of the uniform magnetization is shown for the system of weakly coupled dimers depicted in Fig. 1(a) at various magnetic fields within the partially polarized regime, $h_{c1} < h < h_{c2}$. The anisotropy of the exchange coupling constants, $J'/J = 1/15$, was chosen according to estimates for $TlCuCl_3$. Here J is the strong intradimer and J' is the weak interdimer coupling. In this case, the observed critical fields are well approximated by perturbation theory about the limit of noninteracting dimers, giving $h_{c1} \simeq J - 5J'/2$ and $h_{c2} \simeq J + 5J'$. At ultralow temperatures on the order of J', the magnetization curves of the weakly coupled dimers (solid lines) have a maximum if $h_m < h < h_{c2}$ and a minimum if $h_{c1} < h < h_m$, where $h_m \equiv (h_{c1} + h_{c2})/2$, indicating the onset of a magnetic-field-induced 3D ordering. This feature, emphasized by large filled circles, is absent in the magnetization curves for the noninteracting limit ($J' = 0$), denoted by the dashed lines. While effects of the weak interdimer couplings are clearly negligible at higher temperatures, their relevance at low temperatures is seen in the departure of the solid lines from the dashed lines. In contrast to the mean-field theory of weakly coupled dimers [19], the magnetization is observed to be strongly temperature dependent below the ordering temperature T_c, as shown in Figs. 2(b) and 2(c). On the other hand, the 3D behavior is in qualitative agreement with the recently proposed BEC description of this ordering transition [15].

The dependence of T_c on the applied magnetic field can be extracted from the locus of the extrema in $m(T)$ which were found to be robust to finite size effects for the system sizes considered here [20]. The resulting phase diagram is plotted in Fig. 3 for the ensemble of weakly coupled dimers. As expected from Eq. (1), the transition temperature exhibits a power-law dependence in the vicinity of h_{c1} and h_{c2}. Our best fits, shown in the insets of Fig. 3, yield $\alpha = 2.7 \pm 0.2$ for the lower-field transition and $\alpha = 2.3 \pm 0.2$ in the vicinity of h_{c2}. These critical exponents differ significantly from the value obtained by standard, isotropic Bose-Einstein Hartree-Fock theory, $\alpha_{\mathrm{IBEC}} = 3/2$. It was previously pointed out that some of this deviation may be attributed to shortcomings of the Hartree-Fock description in the critical regions [15].

Another important point is that the dispersion of the spin triplet band is strongly anisotropic [21]. For the case of linearly aligned, weakly coupled dimers the dominant feature in the triplet excitation spectrum is a parabolic bonding band along the strong-coupling direction which becomes populated when the magnetic field is raised beyond h_{c1} [22]. Along the weak-coupling directions the triplet

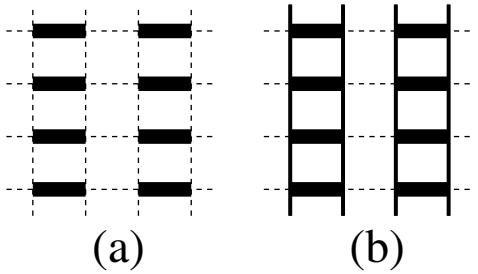

FIG. 1. Layers of anisotropically coupled quantum spins: (a) Weakly coupled dimers and (b) weakly coupled ladders. The strength of the exchange coupling constants is indicated by the thickness of the lines. The 3D interlayer couplings (not shown in the figure) have the same strength as the weakest links (dashed lines) within the planes.

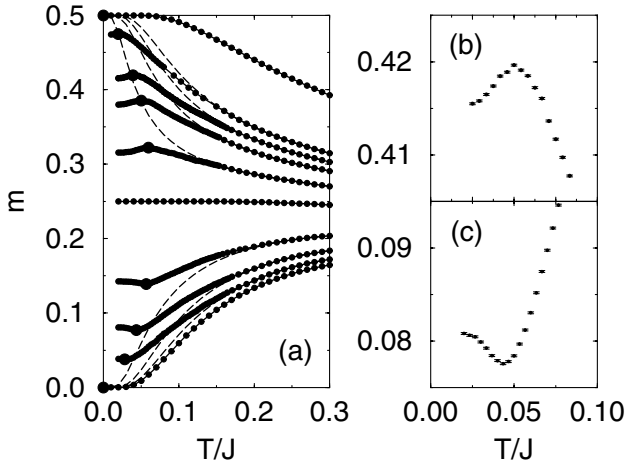

FIG. 2. (a) Temperature dependence of the uniform magnetization in the system of weakly coupled dimers shown in Fig. 1(a). The coupling anisotropy is $J'/J = 1/15$, and the magnetic fields are $h/J = 0.80$, 0.86, 0.90, 0.97, 1.08, 1.17, 1.23, 1.27, 1.32, and 1.37. Extrema in $m(T)$ indicate the onset of 3D ordering and are denoted by enlarged filled circles. Results for the noninteracting ($J'/J = 0$) limit are plotted with dashed lines. (b) Low-temperature regime of $m(T)$ at $h = 1.27J$ and (c) at $h = 0.9J$.

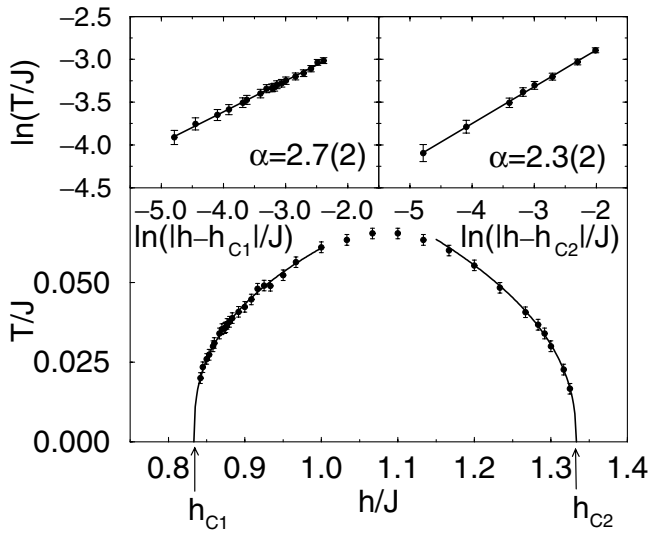

FIG. 3. Phase diagram of the magnetic-field-induced ordering transition in a system of weakly coupled dimers. The scaling exponents in the vicinity of the lower and upper critical fields are extracted from double-logarithmic plots of $T_c(h)$, shown in the insets.

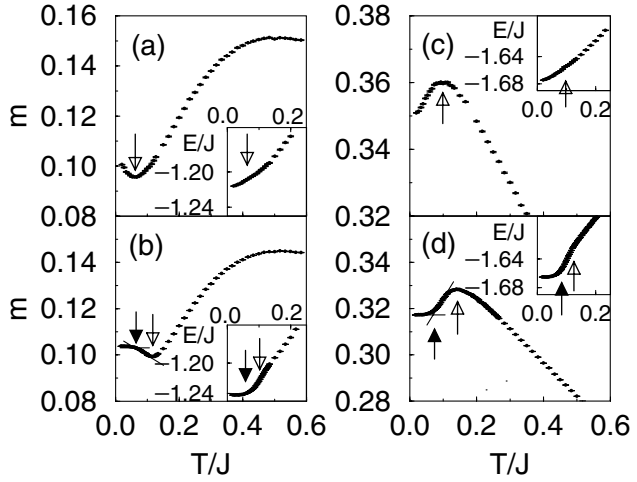

FIG. 4. Low-temperature regime of the uniform magnetization in ladder systems. (a),(c) Isolated two-leg ladders. (b),(d) System of weakly coupled ladders shown in Fig. 1(b). The coupling constants are $J \equiv J_\perp$, $J_\parallel = J/3$, $J' = 0$ for (a) and (c), and $J' = J/15$ for (b) and (d). The applied magnetic fields are $h = 0.83J$ for (a) and (b) and $h = 1.5J$ for (c) and (d). The temperature dependence of the mean free energy is shown in the insets.

excitation spectrum is linear in this regime. Following the BEC Hartree-Fock treatment of [15], a critical exponent $\alpha = 5/2$ is obtained for this case [23]. This anisotropic BEC Hartree-Fock exponent is in better agreement with the QMC simulations than $\alpha_{\mathrm{IBEC}} = 3/2$.

On the other hand, measurements of the lower-field critical exponent in $TlCuCl_3$ give $\alpha \simeq 2.0$ [4] and $\alpha \simeq 2.2$ [15]. This suggests that the generic Heisenberg Hamiltonian which we have studied is not sufficient to accurately model the critical properties of this compound. Reasons for this discrepancy may be found in (i) the much more complex band structure of the spin-triplet excitations in the real material [21,24], (ii) magnetic frustration effects, and (iii) coupling to phonon degrees of freedom.

Let us now turn to the system of weakly coupled two-leg ladders depicted in Fig. 1(b). For the coupling constants chosen in Figs. 4 and 5, the critical magnetic fields are $h_{c1} = 0.61J$ and $h_{c2} = 1.86J$. It has recently been pointed out that this system exhibits extrema in $m(T)$ even in the complete absence of interladder couplings [25]. We can confirm this observation with our simulations of the uniform magnetization, as shown in Figs. 4(a) and 4(c). At magnetic fields slightly above h_{c1} minima occur at low temperatures, whereas maxima are observed at larger magnetic fields close to h_{c2}, indicated by open arrows in Fig. 4. These features indicate the crossover into low-temperature Luttinger liquid behavior in the partially polarized regime, $h_{c1} < h < h_{c2}$ [25]. When the weak interladder couplings are switched on, a second feature, marked by the filled arrows in Figs. 4(b) and 4(d), occurs at still lower temperatures. This is the 3D magnetic ordering transition, also manifested as a change of slope in the mean free energy, as shown in the insets. Measurements of the magnetic specific heat in $Cu_2(C_5H_{12}N_2)_2Cl_4$ indeed show such 3D ordering features at temperatures below the onset of quantum critical behavior [6].

A rich magnetic phase diagram, shown in Fig. 5, can be constructed from these magnetization response functions and shares some of the essential features reported by experiments on $(C_5H_{12}N)_2CuBr_4$ and $Cu_2(C_5H_{12}N_2)_2Cl_4$. At high temperatures (not shown here), the system is

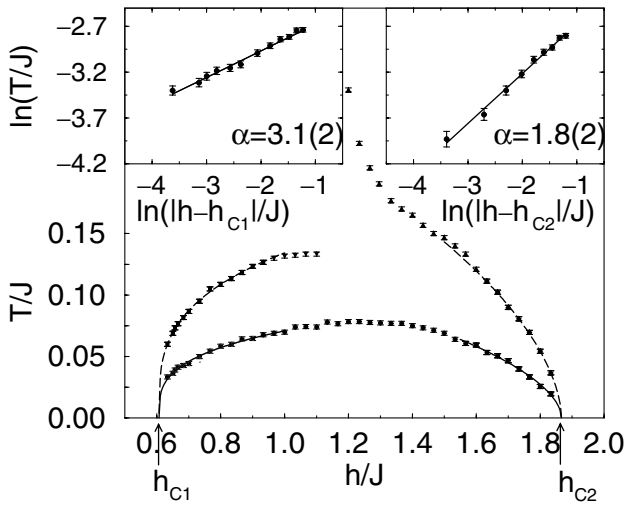

FIG. 5. Magnetic phase diagram of weakly coupled ladders. The upper lines indicate the crossover into a finite-temperature Luttinger liquid regime, also present in isolated two-leg ladders. The lower line marks the magnetic-field-induced 3D ordering transition. The scaling exponents in the vicinity of the lower and upper critical fields are extracted from double-logarithmic plots of $T_c(h)$, shown in the insets.

effectively zero dimensional, with a paramagnetic Curie-law temperature dependence of the magnetic susceptibility. Lowering the temperature, there is a low-field disordered spin liquid regime ($h < h_m$) and a high-field spin-polarized phase ($h > h_m$), where $h_m \approx (h_{c1} + h_{c2})/2$ separates these two regions. The onset of finite-temperature Luttinger liquid behavior is found in the partially spin-polarized regime, $h_{c1} < h < h_{c2}$, at temperatures below $0.13J$ for $J_\parallel = J/3$ [26]. The effective dimensionality of this region is $d = 1$. Finally, 3D ordering occurs at still lower temperatures, as indicated by the lowest transition line in Fig. 5. The scaling exponents extracted from fits of $T_c(h_c)$ to the power law in Eq. (1) are $\alpha = 3.1 \pm 0.2$ at the lower critical field and $\alpha = 1.8 \pm 0.2$ at the upper critical field. These values are quite different from isotropic Bose-Einstein Hartree-Fock theory, suggesting that a successful effective theory needs to account more accurately for the quantum dynamics of the lower-dimensional subsystems.

In summary, we have studied the magnetic phase diagram and the critical behavior in models of weakly coupled quantum spin liquids. Using the stochastic series expansion QMC method, we were able to reach sufficiently low temperatures such that magnetic-field-induced 3D ordering could be observed. The scaling exponents depend strongly on the dimensionality and on the quantum dynamics of the subsystems, Heisenberg dimers and ladders, which reflect the strongly anisotropic dispersion of the triplet excitation bands. While this study has concentrated on the fundamental features of generic model Hamiltonians, much more detailed models are clearly needed to account for the specific scaling properties observed in real materials.

We thank N. Cavadini, A. Honecker, B. Normand, M. Oshikawa, G. S. Uhrig, and X. Wang for useful discussions, and we acknowledge financial support by the Department of Energy, Grant No. DE-FG03-01ER45908 (S. H., S. W.), and the National Science Foundation, Grant No. PHY-0070333 (M. O.).

[1] T. Giamarchi and A. M. Tsvelik, Phys. Rev. B **59**, 11 398 (1999).
[2] S. Wessel and S. Haas, Eur. Phys. J. B **16**, 393 (2000); Phys. Rev. B **62**, 316 (2000).
[3] A. Oosawa, M. Ishii, and H. Tanaka, J. Phys. Condens. Matter **11**, 265 (1999).
[4] H. Tanaka, A. Oosawa, T. Kato, H. Uekusa, Y. Ohashi, K. Kakurai, and A. Hoser, cond-mat/0101276.
[5] G. Chaboussant, Y. Fagot-Revurat, M. H. Julien, M. E. Hanson, C. Berthier, M. Horvatić, L. P. Lévy, and O. Piovesana, Phys. Rev. Lett. **80**, 2713 (1998); Eur. Phys. J. B **6**, 167 (1998).
[6] R. Calemczuk, J. Riera, D. Poilblanc, J.-P. Boucher, G. Chaboussant, L. Levy, and O. Piovesana, Eur. Phys. J. B **7**, 171 (1999).
[7] P. R. Hammar, D. H. Reich, C. Broholm, and F. Trouw, Phys. Rev. B **57**, 7846 (1998).
[8] H. Mayaffre, M. Horvatić, C. Berthier, M.-H. Julien, P. Ségransan, L. Lévy, and O. Piovesana, Phys. Rev. Lett. **85**, 4795 (2000).
[9] R. D. Willett, C. Dwiggins, R. F. Kruh, and R. E. Rundle, J. Chem. Phys. **38**, 2429 (1963).
[10] K. Takatsu, W. Shiramura, and H. Tanaka, J. Phys. Soc. Jpn. **66**, 1611 (1997).
[11] W. Shiramura, K. Takatsu, H. Tanaka, K. Kamishima, M. Takahashi, H. Mitamura, and T. Goto, J. Phys. Soc. Jpn. **66**, 1900 (1997).
[12] M. B. Stone, J. Rittner, Y. Chen, H. Yardimci, D. H. Reich, C. Broholm, D. V. Ferraris, and T. Lectka, cond-mat/0103023.
[13] B. R. Patyal, B. L. Scott, and R. D. Willett, Phys. Rev. B **41**, 1657 (1990).
[14] B. C. Watson, V. N. Kotov, M. W. Meisel, D. W. Hall, G. E. Granroth, W. T. Montfrooij, S. E. Nagler, D. A. Jensen, R. Backov, M. A. Petruska, G. E. Fanucci, and D. R. Talham, Phys. Rev. Lett. **86**, 5168 (2001).
[15] T. Nikuni, M. Oshikawa, A. Oosawa, and H. Tanaka, Phys. Rev. Lett. **84**, 5868 (2000).
[16] T. Nikuni and H. Shiba, J. Phys. Soc. Jpn. **64**, 3471 (1995).
[17] A. Honecker, J. Phys. Condens. Matter **11**, 4697 (1999).
[18] A. W. Sandvik, Phys. Rev. B **59**, R14 157 (1999).
[19] M. Tachiki and T. Yamada, J. Phys. Soc. Jpn. **28**, 1413 (1970).
[20] In practice, we monitor the numerical derivative of $m(T)$ to obtain a more precise location of $T_c(h)$.
[21] N. Cavadini, G. Heigold, W. Henggeler, A. Furrer, H.-U. Güdel, K. Krämer, and H. Mutka, Phys. Rev. B **63**, 172414 (2001).
[22] I. Affleck, Phys. Rev. B **43**, 3215 (1991).
[23] V. Bagnato and D. Kleppner, Phys. Rev. A **44**, 7439 (1991).
[24] A. Oosawa, T. Kato, H. Tanaka, H. Uekusa, Y. Ohashi, K. Nakajima, M. Nishi, and K. Kakurai, cond-mat/0004108.
[25] X. Wang and L. Yu, Phys. Rev. Lett. **84**, 5399 (2000).
[26] Zero-temperature Luttinger liquid behavior is observed only for vanishing interladder couplings.